# Gold and Silver Nanoparticles Functionalized by the Adsorption of Dialkyl Disulfides

Lon A. Porter, Jr.,[†] David Ji,[†] Sarah L. Westcott,[‡] Michael Graupe,[†] Roman S. Czernuszewicz,[†] Naomi J. Halas,[‡] and T. Randall Lee*[,†]

*Department of Chemistry, University of Houston, Houston, Texas 77204-5641, and Department of Electrical and Computer Engineering, Rice University, Houston, Texas 77005*

*Received July 13, 1998. In Final Form: October 8, 1998*

The formation of three-dimensional self-assembled monolayers (3-D SAMs) generated by the adsorption of *n*-octadecyl disulfide onto colloidal gold and silver nanoparticles is described. The functionalized nanoparticles were characterized by solubility, transmission electron microscopy, ultraviolet−visible spectroscopy, $^1$H nuclear magnetic resonance spectroscopy, surface-enhanced Raman spectroscopy, Fourier transform infrared spectroscopy, and X-ray photoelectron spectroscopy. On gold nanoparticles, this new functionalization method affords crystalline 3-D SAMs that are indistinct from those prepared by the analogous adsorption of *n*-octadecanethiol. On silver nanoparticles, however, the films derived from *n*-octadecyl disulfide appear to be somewhat less crystalline than those prepared similarly from *n*-octadecanethiol. The origin of this difference is briefly explored and discussed.

## Introduction

Self-assembled monolayers (SAMs) generated by the adsorption of organic molecules onto two-dimensional (2-D) surfaces represent an ever expanding field of research due to their potential use in applications such as corrosion prevention,[1] lubrication,[1] electrical conduction,[2−5] adhesion,[6] and catalysis.[7] Perhaps the most thoroughly investigated SAMs are those generated by the adsorption of organic thiols or disulfides onto flat surfaces of gold.[8−14] The adsorption of these species onto other metals such as silver and copper is somewhat hindered by the facile oxidation of the surfaces of these metals.[13−16] One of the current goals of this area of research is to use SAMs to pacify the surfaces of the metals, thereby affording protection against corrosion and degradation.[17,18] SAMs have drawn special attention because the methodology is simple,[11] and the resultant films are densely packed, highly ordered, and largely free of defects.[9] Furthermore, the ability to employ a wide variety of structurally diverse organosulfur adsorbates offers great versatility in thin-film design.[12]

Recent years have also witnessed an explosive growth in studies focusing on the adsorption of molecular species onto colloidal particles of gold, silver, copper, and platinum.[19−27] These functionalized nanoparticles have found use in a wide range of technologies.[28−32] The sol particle immunoassay (SPIA), for example, exploits colloid aggregation to monitor the interaction between an antibody or antigen bound to a colloid and its binding partner.[28] Surface-passivated metal colloids serve as useful materials for the manufacture of microelectronics.[29] Other applications include colloid-modified electrodes,[30] colored labeling agents for electron and visible microscopy,[31] and quantum-confinement materials.[32]

The development of a two-phase liquid/liquid route[33,34] to *n*-alkanethiol-derivatized metal nanoparticles has

* To whom correspondence should be addressed. E-mail: trlee@uh.edu.

[†] University of Houston.

[‡] Rice University.

(1) Adamson, A. W. *Physical Chemistry of Surfaces*; Wiley: New York, 1976.

(2) Kuhn, H.; Möbius, D. *Techniques of Organic Chemistry*; Wiley: New York, 1972.

(3) Polymeropoulos, E. E.; Sagiv, J. *J. Chem. Phys.* **1978**, *69*, 1836.

(4) Sugi, M.; Fukui, T.; Lizima, S. *Phys Rev. B* **1978**, *18*, 725.

(5) Furtlehner, J. P.; Messier, J. *Thin Solid Films* **1980**, *68*, 233.

(6) Waldbillig, R. C.; Robertson, J. D.; McIntosh, T. *J. Biochim. Biophys. Acta* **1976**, *448*, 1.

(7) Kornberg, R. D.; McConnell, H. M. *Biochemistry* **1971**, *10*, 1111.

(8) Nuzzo, R. G.; Allara, D. L. *J. Am. Chem. Soc.* **1983**, *105*, 4481.

(9) Dubois, L. H.; Nuzzo, R. G. *Annu. Rev. Phys. Chem.* **1992**, *43*, 437.

(10) Bain, C. D.; Troughton, E. B.; Tao, Y.-T.; Evall, J.; Whitesides, G. M.; Nuzzo, R. G. *J. Am. Chem. Soc.* **1989**, *111*, 321.

(11) Bain, C. D.; Whitesides, G. M. *Angew. Chem., Int. Ed. Engl.* **1989**, *28*, 506.

(12) Whitesides, G. M.; Laibinis, P. E. *Langmuir* **1990**, *6*, 87.

(13) Ulman, A. *An Introduction to Ultrathin Organic Films*; Academic: New York, 1991.

(14) Ulman, A. *Chem. Rev.* **1996**, *96*, 1533.

(15) Walczak, M. M.; Chung, C.; Stole, S. M.; Widrig, C. A.; Porter, M. D. *J. Am. Chem. Soc.* **1991**, *113*, 2370 and references therein.

(16) Laibinis, P. E.; Whitesides, G. M.; Allara, D. L.; Tao, Y.-T.; Parikh, A. N.; Nuzzo, R. G. *J. Am. Chem. Soc.* **1991**, *113*, 7152 and references therein.

(17) Jennings, G. K.; Laibinis, P. E. *J. Am. Chem. Soc.* **1997**, *119*, 5208.

(18) Zamborini, F. P.; Campbell, J. K.; Crooks, R. M. *Langmuir* **1998**, *14*, 640.

(19) Lee, P. C.; Meisel, D. *J. Phys. Chem.* **1982**, *86*, 3391.

(20) Xu, H.; Tseng, C.-H.; Vickers, T. J.; Mann, C. K.; Schlenoff, J. B. *Surf. Sci.* **1994**, *311*, L707−711.

(21) Grabar, K. C.; Allison, K. J.; Baker, B. E.; Bright, R. M.; Brown, K. R.; Freeman, R. G.; Fox, A. P.; Keating, C. D.; Musick, M. D.; Natan, M. J. *Langmuir* **1996**, *12*, 2353.

(22) Weisbecker, C. S.; Meritt, M. V.; Whitesides, G. M. *Langmuir* **1996**, *12*, 3763.

(23) Leff, D. V.; Brandt, L.; Heath, J. R. *Langmuir* **1996**, *12*, 4723.

(24) Sarathy, K. V.; Raina, G.; Yadav, R. T.; Kulkarni, G. U.; Rao, C. N. R. *J. Phys. Chem. B* **1997**, *101*, 9876.

(25) Brown, K. R.; Natan, M. J. *Langmuir* **1998**, *14*, 726−728.

(26) Ingram, R. S.; Hostetler, M. J.; Murray, R. W.; Schaaff, T. G.; Khoury, J. T.; Whetten, R. L.; Bigioni, T. P.; Guthrie, D. K.; First, P. N. *J. Am. Chem. Soc.* **1997**, *119*, 9279.

(27) Green, S. J.; Stokes, J. J.; Hostetler, M. J.; Pietron, J.; Murray, R. W. *J. Phys. Chem. B* **1997**, *101*, 2663.

(28) Van Erp, R.; Gribnau, T. C. J.; Van Sommeren, A. P. G.; Bloemers, H. P. J. *J. Immunoassay* **1990**, *11*, 31.

(29) Schon, G.; Simon, U. *Colloid Polym. Sci.* **1995**, *273*, 101.

(30) Dorn, A.; Katz, E.; Willner, I. *Langmuir* **1995**, *11*, 1313.

(31) Beesley, J. E. *Colloidal Gold: A New Perspective for Cytochemical Marking; Royal Microscopical Society Microscopy Handbook 17*; Oxford University Press: Oxford, U.K., 1989.

(32) Hanna, A. E.; Tinkham, M. *Phys. Rev. B* **1991**, *44*, 5919.

(33) Brust, M.; Walker, M.; Bethell, D.; Schiffrin, D. J.; Whyman, R. *J. Chem. Soc., Chem. Commun.* **1994**, 801.

10.1021/la980870i CCC: $15.00 
Published on Web 11/19/1998

further advanced this area of research.[35−50] Functionalized nanoparticles generated in this manner exist as dark-brown/black solids that are easy to isolate, stable in air, and soluble in a wide range of organic solvents. These features permit facile manipulation and characterization using a variety of techniques such as transmission electron microscopy (TEM),[40,48−50] ultraviolet−visible (UV−vis) spectroscopy,[49,50] nuclear magnetic resonance (NMR) spectroscopy,[35−39,49] surface-enhanced Raman spectroscopy (SERS),[19,20] Fourier transform infrared (FTIR) spectroscopy,[33−35,37,39,46−50] and X-ray photoelectron spectroscopy (XPS).[22,50,72]

While it has been demonstrated that SAMs on 2-D metal surfaces (2-D SAMs) can be generated from either thiols or disulfides to yield films having virtually indistinguishable differences,[51−53] few, if any, studies have explored the use of disulfides to generate SAMs on colloidal surfaces (3-D SAMs). Previous research appears to be limited exclusively to the adsorption of thiols, amines, and silanes.[35−50] Disulfides offer several attractive features for the preparation of 3-D SAMs. First, the use of unsymmetrical disulfides having two distinct functional groups at the molecular termini (RSSR′) offers the possibility of generating mixed SAMs possessing a homogeneous distribution of functional groups.[54] Studies of nanoparticles that expose these multicomponent interfaces might, for example, permit the modeling of complex biological systems (e.g., cell−cell interactions). Second, the use of unsymmetrical disulfides possessing two distinct chain lengths (RSSR″) offers the possibility of generating 3-D SAMs with designed molecular "roughnesses". This feature might prove useful in manipulating the interactions between nanoparticles by controlling the degree of interdigitation of the molecular tail groups.[45] Third, disulfides can be used to generate functionalized 3-D SAMs in cases where the $\omega$-functional group is incompatible with, for example, thiols or amines.[55,56]

Herein, we describe the preparation, isolation, and characterization of 3-D SAMs generated by the adsorption of *n*-octadecyl disulfide, $(C_{18}S)_2$, onto the surfaces of gold and silver nanoparticles. On the gold nanoparticles, we find that these disulfide-derived 3-D SAMs are well ordered, highly crystalline, and indistinct from those prepared in analogous fashion from the adsorption of *n*-octadecanethiol. On the silver nanoparticles, however, the films generated from the disulfide, while still well ordered and highly crystalline, appear to be somewhat less crystalline than those generated from the thiol.

## Experimental Section

**Materials.** The following reagents were purchased from the indicated suppliers and used without modification: $HAuCl_4$ (Strem), $AgNO_3$ (Strem), $(C_8H_{17})_4NBr$ (Aldrich), $NaBH_4$ (EM Sciences), and *n*-octadecanethiol (Aldrich). A sample of *n*-octadecyl disulfide was prepared by oxidation of the thiol with iodine. Absolute ethanol was purchased from McKormick Distilling Co.; Omnisolve grade toluene and hexane were purchased from EM Sciences. All other solvents and materials were obtained from commercial sources and used without modification.

**Preparation of 3-D SAMs on Gold Nanoparticles by the Adsorption of $(C_{18}S)_2$.** A 20.0 mL aliquot of a $2.54 \times 10^{-2}$ M aqueous solution of $HAuCl_4$ (0.508 mmol) was transferred to an empty 250 mL round-bottomed flask.[57] To this vigorously stirred solution, 15.0 mL of a $7.52 \times 10^{-2}$ M solution of $(C_8H_{17})_4NBr$ (1.13 mmol) in toluene was added. Stirring was allowed to proceed for at least 15 min to ensure complete transfer of the gold into the organic layer. This transfer could be followed visually by observing the disappearance of the faint yellow coloration of the aqueous phase and the concomitant appearance of a reddish-orange coloration of the organic phase. A 10.0 mL aliquot of a $8.58 \times 10^{-3}$ M solution of $(C_{18}S)_2$ (0.0858 mmol) in toluene was added dropwise to the vigorously stirred organic phase. We chose a one to three molar ratio of sulfur to metal to produce functionalized nanoparticles sufficiently large for facile manipulation and ready imaging by TEM. A 50.0 mL aliquot of a $1.12 \times 10^{-1}$ M aqueous solution of $NaBH_4$ (5.58 mmol) was then added dropwise over 30 min. With the addition of only a few drops of the $NaBH_4$ solution, the color of the organic phase changed immediately (ca. 30 s) from reddish-orange to dark violet. The mixture was allowed to stir for approximately 12 h. The organic phase was concentrated to ca. 3 mL using a rotary evaporator, and the mixture was diluted with 300 mL of ethanol and stored at −50 °C overnight. The functionalized gold nanoparticles were then collected as a brownish black precipitate by filtration through a 2.5 $\mu$m polypropylene membrane filter (Millipore). The precipitate was washed briefly with acetone (1 × 10 mL) and then exhaustively with ethanol (3 × 400 mL).

**Preparation of 3-D SAMs on Gold Nanoparticles by the Adsorption of $C_{18}SH$.** The procedure detailed above was employed with the substitution of $C_{18}SH$ for $(C_{18}S)_2$. To maintain a constant ratio of sulfur to gold (i.e., 1:3), we used 10.0 mL of a $1.71 \times 10^{-2}$ M solution of the thiol (0.171 mmol) in toluene. Upon the addition of $NaBH_4$, the rapid change in the color of the solution from reddish-orange to dark violet was similar to that observed in the procedure employing the disulfide.

**Preparation of 3-D SAMs on Silver Nanoparticles by the Adsorption of $(C_{18}S)_2$.** A 20.0 mL aliquot of a $2.50 \times 10^{-2}$ M aqueous solution of $AgNO_3$ (0.500 mmol) was transferred to an empty 250 mL round-bottomed flask.[57] To this vigorously stirred solution, 15.0 mL of a $7.40 \times 10^{-2}$ M solution of $(C_8H_{17})_4$-

(34) Brust, M.; Fink, J.; Bethell, D.; Schiffrin, D. J.; Kiely, C. J. *J. Chem. Soc., Chem. Commun.* **1995**, 1655.
(35) Leff, D. V.; Ohara, P. C.; Heath, J. R.; Gelbart, W. M. *J. Phys. Chem.* **1995**, *99*, 7036.
(36) Terrill, R. H.; Postlethwaite, T. A.; Chen, C.-H.; Poon C.-D.; Terzis, A.; Chen, A.; Hutchinson, J. E.; Clark, M. R.; Wignall, G.; Londono, J. D.; Superfine, R.; Falvo, M.; Johnson, C. S.; Samulski, E. T.; Murray, R. W. *J. Am. Chem. Soc.* **1995**, *117*, 12537.
(37) Hostetler, M. J.; Green, S. J.; Stokes, J. J.; Murray, R. W. *J. Am. Chem. Soc.* **1996**, *118*, 4212.
(38) Badia, A.; Demers, L.; Dickinson, L.; Morin, F. G.; Lennox, R. B.; Reven, L. *J. Am. Chem. Soc.* **1997**, *119*, 11104.
(39) Templeton, A. C.; Hostetler, M. J.; Kraft, C. T.; Murray, R. W. *J. Am. Chem. Soc.* **1998**, *120*, 1906.
(40) Grabar, K. C.; Brown, K. R.; Keating, C. D.; Stranick, S. J.; Tang, S.-L.; Natan, M. J. *Anal. Chem.* **1997**, *69*, 471.
(41) Heath, J. R.; Knobler, C. M.; Leff, D. V. *J. Phys. Chem. B* **1997**, *101*, 189.
(42) Badia, A.; Gao, W.; Singh, S.; Demera, L.; Cuccia, L.; Reven, L. *Langmuir* **1996**, *12*, 1262.
(43) Grabar, K. C.; Smith, P. C.; Musick, M. D.; Davis, J. A.; Walter, D. G.; Jackson, M. A.; Guthrie, A. P.; Natan, M. *J. Am. Chem. Soc.* **1996**, *118*, 1149.
(44) Wang, Z. L.; Harfenist, S. A.; Whetten, R. L.; Bentley, J.; Evans, N. D. *J. Phys. Chem. B* **1998**, *102*, 3068.
(45) Badia, A.; Singh, S.; Demers, L.; Cuccia, L.; Brown, G. R.; Lennox, R. B. *Chem. Eur. J.* **1996**, *2*, 359.
(46) Hostetler, M. J.; Stokes, J. J.; Murray, R. W. *Langmuir* **1996**, *12*, 3604.
(47) Ingram, R. S.; Hostetler, M. J.; Murray, R. W. *J. Am. Chem. Soc.* **1997**, *119*, 9175.
(48) Badia, A.; Cuccia, L.; Demers, L.; Morin, F.; Lennox, R. B. *J. Am. Chem. Soc.* **1997**, *119*, 2682.
(49) Hostetler, M. J.; Wingate, J. E.; Zhong, C.-J.; Harris, J. E.; Vachet, R. W.; Clark, M. R.; Londono, J. D.; Green, S. J.; Stokes, J. J.; Wignall, G. D.; Glish, G. L.; Porter, M. D.; Evans, N. D.; Murray, R. W. *Langmuir* **1998**, *14*, 17.
(50) Kang, S. Y.; Kim, K. *Langmuir* **1998**, *14*, 226.
(51) Nuzzo, R. G.; Fusco, F. A.; Allara, D. L. *J. Am. Chem. Soc.* **1987**, *109*, 2358.
(52) Bain, C. D.; Biebuyck, H. A.; Whitesides, G. M. *Langmuir* **1989**, *5*, 723.
(53) Biebuyck, H. A.; Bain, C. D.; Whitesides, G. M. *Langmuir* **1994**, *10*, 1825.
(54) Schönherr, H.; Ringsdorf, H. *Langmuir* **1996**, *12*, 3891.
(55) Gaertner, V. R. *J. Heterocycl. Chem.* **1971**, *8*, 519.
(56) Hassner, A. *Small Ring Heterocycles. Part 1.*; Wiley: New York, 1983.
(57) All glassware was washed with Aqua Regia, throughly rinsed with distilled water and acetone, and dried prior to use.

NBr (1.11 mmol) in toluene was added. Stirring was allowed to proceed for at least 15 min to ensure complete transfer of the silver into the organic layer. A 10.0 mL aliquot of a $8.40 \times 10^{-3}$ M solution of $(C_{18}S)_2$ (0.0840 mmol) in toluene was added dropwise to the vigorously stirred organic phase. A 50.0 mL aliquot of a 0.110 M aqueous solution of $NaBH_4$ (5.50 mmol) was then added dropwise over 30 min. With the addition of only a few drops of the $NaBH_4$ solution, the color of the organic phase changed from colorless to tan and then to dark brown after ca. 5 min (i.e., before the addition was complete). The mixture was allowed to stir for approximately 12 h. The organic phase was concentrated to ca. 3 mL using a rotary evaporator, and the mixture was diluted with 300 mL of ethanol and stored at −50 °C overnight. The functionalized silver nanoparticles were then collected as a brownish black precipitate by filtration through a 2.5 $\mu$m polypropylene membrane filter (Millipore). The precipitate was washed briefly with acetone (1 × 10 mL) and then exhaustively with ethanol (3 × 400 mL).

**Preparation of 3-D SAMs on Silver Nanoparticles by the Adsorption of $C_{18}SH$.** These SAMs were prepared using the above procedure, but employed the thiol rather than the disulfide. To maintain a constant molar ratio of sulfur to silver (1:3), we used 10.0 mL of a $1.67 \times 10^{-2}$ M solution of $C_{18}SH$ (0.167 mmol) in toluene. In these preparations, the change of the color to brown induced by the addition of $NaBH_4$ was a bit more rapid (ca. 2 min compared to 5 min).

**Characterization Methods.** TEM images were collected on a JEOL JEM-2010 electron microscope operating at an accelerating bias voltage of 200 kV. Samples were prepared by evaporating a film of nanoparticles onto a 200 mesh copper grid, which was coated with a carbon support film. UV−vis spectra were measured using a Perkin-Elmer Lambda 3B spectrophotometer. The experimental data were corrected for the background absorbance of the solvent (benzene). NMR spectra were recorded on a General Electric QE-300 spectrometer operating at 300 MHz. The data were collected using $CDCl_3$ as the solvent and internally referenced to $\delta$ 7.26 ppm. Raman spectra of the gold samples were obtained by excitation with a Coherent K-2 $Kr^+$ ion laser at 647.1 nm. The typical applied laser powers were 100−200 mW with a 10 $cm^{-1}$ slit width. Scattered photons were collected via backscattering from spinning NMR tubes.[58] Raman specta for the silver samples were obtained by excitation with a Coherent 90-6 $Ar^+$ ion laser at 514.5 nm. The typical applied laser powers were 100−200 mW with a 4 $cm^{-1}$ slit width. Scattered photons were collected via backscattering geometry from rotating solid samples in pressed KCl pellets.[58] The scattered radiation was dispersed by a Spex 1403 double monochromator equipped with 1800 grooves/mm holographic gratings and detected by a cooled Hamamatsu 928 photomultiplier tube.[59] The data were collected digitally using a Spex DM3000 microcomputer at 0.5 $cm^{-1}$ increments and 1 s integration time per data point. To improve the signal-to-noise ratio, 5−10 scans were collected on each sample. Infrared spectra were obtained on a Nicolet MAGNA-IR 860 Fourier transform spectrometer. Spectra were recorded using 16 scans with a spectral resolution of 1 $cm^{-1}$. Samples of the nanoparticles in solution were analyzed using carbon tetrachloride ($CCl_4$) as the solvent. Samples of the nanoparticles in the solid state were prepared by placing a drop of the nanoparticle solution onto a silicon wafer and allowing the solvent ($CCl_4$) to evaporate. XPS data were obtained on a PHI 5700 X-ray photoelectron spectrometer using an Al K$\alpha$ X-ray source. Samples were collected on the surface of a 2.5 $\mu$m polypropylene filter and washed exhaustively with ethanol before analysis.

## Results and Discussion

**I. 3-D SAMs on Gold Nanoparticles. Solubilities of $(C_{18}S)_2$/Au Nanoparticles.** The gold nanoparticles synthesized using the dialkyl disulfide-based procedure dissolved readily in organic solvents such as hexane, cyclohexane, benzene, $CCl_4$, and THF. The particles could be repeatedly precipitated and redissolved without loss of solubility. Since bare gold colloids are typically insoluble in organic solvents and tend to flocculate irreversibly upon drying,[33] the observed solubilities and dissolution behavior strongly suggest that the dialkyl disulfides form at least partial 3-D SAMs on the surfaces of the gold nanoparticles.

**TEM Images of $(C_{18}S)_2$/Au Nanoparticles.** Imaging by TEM is one of the primary tools used to characterize metal nanoparticles.[40,48−50] Figure 1a provides a TEM image of the dialkyl disulfide-coated gold nanoparticles produced using the procedure detailed above. The particles are roughly spherical and comparable in appearance to previously reported alkanethiol-coated gold nanoparticles.[33] A random sampling of 100 of the disulfide-functionalized nanoparticles afforded the histogram shown in Figure 1b, which illustrates that the particles range in size from 1.0 to ca. 4.0 nm (with those having diameters of 1.5 to 3.0 nm occurring most frequently). The histogram in Figure 1c demonstrates that the analogous alkanethiol-based procedure yields a similar size distribution. Since both adsorbates afford nanoparticles having similar sizes and morphologies, we infer that the constant ratio of sulfur to gold (1:3) employed in the syntheses is a major factor influencing the growth of gold nanoparticles.[35]

**UV−vis Spectroscopy of $(C_{18}S)_2$/Au Nanoparticles.** UV−vis spectra of the disulfide-coated gold nanoparticles exhibited a strong absorption at 520 nm corresponding to the gold plasmon resonance (data not shown).[60] The observed wavelength of absorption is consistent with that reported for gold nanoparticles functionalized by the adsorption of alkanethiols.[35]

**$^1$H NMR Spectroscopy of $(C_{18}S)_2$/Au Nanoparticles and Nanoparticle Formation.** In the present work, we used solution-phase $^1$H NMR spectroscopy to examine the disulfide-functionalized gold nanoparticles. The use of $^1$H NMR spectroscopy in the characterization of 3-D SAMs on metal nanoparticles permits a facile scan for the presence of any unbound adsorbates, which can often be difficult to remove completely in nanoparticle syntheses.[45] Spectra obtained in $CDCl_3$ showed three broad resonances at $\delta$ 0.8−0.9, 1.2−1.4, and 1.5−1.7 ppm (data not shown). No free alkanethiol (e.g., $\delta$ 2.50 ppm) or dialkyl disulfide (e.g., $\delta$ 2.67 ppm) was detected. These observations suggest that the hydrocarbon species derived from the disulfide are attached to the surface of the colloid via the sulfur atom.[45] Furthermore, the spectra are fully consistent with those reported in the literature for alkanethiol-functionalized gold nanoparticles.[47]

Since disulfides can be readily reduced to thiols, it seemed plausible that $NaBH_4$ might at least partially reduce *n*-octadecyl disulfide to *n*-octadecanethiol during the two-phase synthesis. If this reduction were to happen, the transient thiol might then serve as the active species forming the 3-D SAMs. To test for this possibility, we performed the two-phase reduction as described above but omitted the addition of $HAuCl_4$. Separation of the organic and aqueous layers followed by evaporation of the organic phase yielded a white residue. Acidification of the aqueous phase followed by extraction with hexane (3 × 100 mL) and evaporation to dryness yielded a hardly visible white residue. After dissolving each residue in $CDCl_3$, we examined the resulting solutions by $^1$H NMR spectroscopy. While *n*-octadecyl disulfide was readily detected in the former sample, and tetraoctylammonium bromide was readily detected in both of the samples, neither sample exhibited resonances characteristic of *n*-octadecanethiol (e.g., $\delta$ 2.5 ppm). Since these studies

(58) Czernuszewicz, R. S. *Appl. Spectrosc.* **1986**, 40, 571.
(59) Czernuszewicz, R. S. In *Methods in Molecular Biology*; Jones, C.; Mulloy, B.; Thomas, A. H.; Eds.; Humana: Totowa, NJ, 1993.
(60) Henglein, A. *J. Phys. Chem.* **1993**, *97*, 5457.

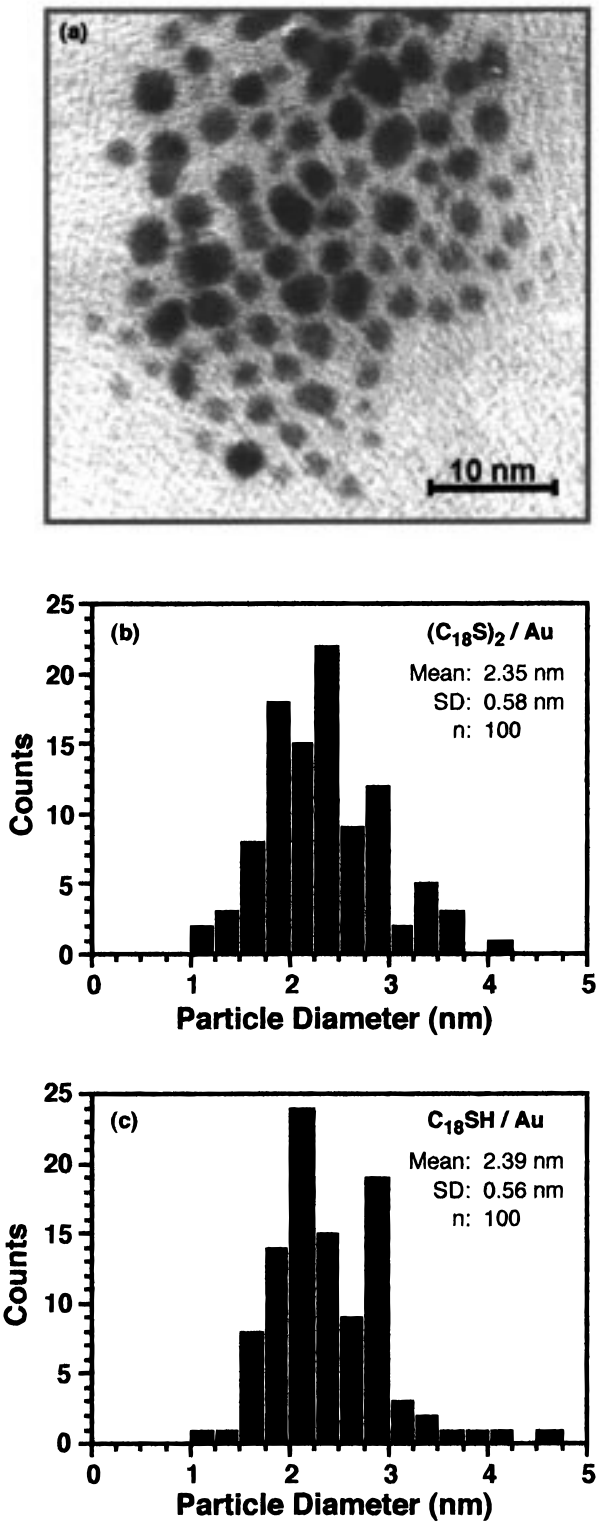


**Figure 1.** (a) TEM image of gold nanoparticles functionalized with *n*-octadecyl disulfide. (b) TEM-derived nanoparticle size distribution for gold nanoparticles functionalized with *n*-octadecyl disulfide. (c) TEM-derived nanoparticle size distribution for gold nanoparticles functionalized with *n*-octadecanethiol.

provide only indirect evidence that the reducing conditions employed here are insufficient to reduce the disulfide to the thiol, we are hesitant to conclude from these observations that the active species in the disulfide-based formation of 3-D SAMs on gold is the disulfide itself rather than the corresponding thiol. We note, however, that analogous studies on silver nanoparticles (vide infra) provide much

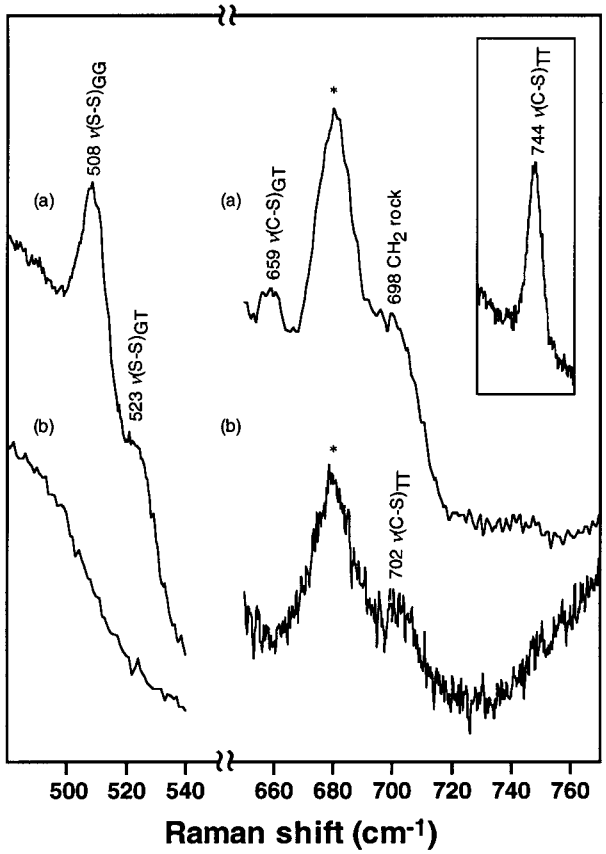


**Figure 2.** Raman spectra in the 480−550 and 650−770 $cm^{-1}$ region for solution ($C_6H_6$) samples of (a) free *n*-octadecyl disulfide and (b) gold nanoparticles functionalized with *n*-octadecyl disulfide. The insert shows the Raman scattering of the former sample in the range of 720−760 $cm^{-1}$ obtained with 40 scans at 250 mW at a resolution of 0.2 $cm^{-1}$ $s^{-1}$. The asterisk indicates the solvent band (benzene).

stronger support for the direct, exclusive participation of the disulfide. Consequently, we feel confident that the disulfide is also the active species involved here.

**Raman Spectra of $(C_{18}S)_2$/Au and $C_{18}SH$/Au Nanoparticles.** Raman spectroscopy has proven to be a useful tool in the characterization of 3-D SAMs on gold.[19,20] Bonding of the disulfide to the surface of gold nanoparticles can be followed by monitoring the loss of the S−S stretch (500−540 $cm^{-1}$) and shifts of the C−S stretches (600−750 $cm^{-1}$). Figure 2 shows the Raman spectra of *n*-octadecyl disulfide and the 3-D SAMs produced from the adsorption of *n*-octadecyl disulfide on the gold nanoparticles. Unadsorbed (or free) *n*-octadecyl disulfide exhibits bands at 523 and 508 $cm^{-1}$ (Figure 2a), which arise from the $\nu$(S−S) stretches of the gauche−trans (GT) and gauche−gauche (GG) conformations, respectively.[61−64] Upon adsorption, these two bands disappear, and a new band appears at 702 $cm^{-1}$ (Figure 2b). This new band also appears upon the adsorption of octadecanethiol onto the gold nanoparticles (data not shown).

We assign the 702 $cm^{-1}$ band, which shifts from 744 $cm^{-1}$ for the free disulfide (Figure 2, inset), as the $\nu$(C−S) stretch of the trans−trans (TT) conformer. This assignment is consistent with those in the literature for 3-D

(61) Sheppard, N. *Trans. Faraday Soc.* **1950**, *46*, 429.
(62) Sandroff, C. J.; Garoff, S.; Leung, K. P. *Chem. Phys. Lett.* **1983**, *96*, 547.
(63) Bryant, M. A.; Pemberton, J. E. *J. Am. Chem. Soc.* **1991**, *113*, 3629.
(64) Bryant, M. A.; Pemberton, J. E. *J. Am. Chem. Soc.* **1991**, *113*, 8284.

SAMs on gold derived from alkanethiols.[64] Accordingly, we conclude that these data, when combined with the observed loss of the S−S stretches, provide the first direct support for the disulfide-based covalent functionalization of gold nanoparticles. Furthermore, the loss of the $\nu$(C−S) GT band at ∼659 $cm^{-1}$ upon adsorption suggests that the 3-D SAMs consist of highly ordered alkyl chains in the region near the sulfur headgroup.[62,64]

**IR Spectroscopy of $(C_{18}S)_2$/Au and $C_{18}SH$/Au Nanoparticles.** Remarkably detailed insight into the structures of 3-D SAMs on metal nanoparticles can be obtained from infrared spectroscopy.[33−35,37,39,46−50] Examination, for example, of the C−H and C−C stretching regions provides information regarding the orientation, order, and packing of these thin films. Analysis of the C−H stretching region is perhaps the most informative. Consider, for example, the C−H stretches of a model hydrocarbon such as polyethylene in which the antisymmetric ($\nu_{as}$) and symmetric ($\nu_s$) methylene stretches appear as relatively broad bands at $\nu_{as}(CH_2) = 2928$ $cm^{-1}$ and $\nu_s(CH_2) = 2856$ $cm^{-1}$ when the polymer is dissolved in solution (i.e., randomly oriented and poorly packed). In crystalline form, however, these bands sharpen and shift to $\nu_{as}(CH_2) = 2920$ $cm^{-1}$ and $\nu_s(CH_2) = 2850$ $cm^{-1}$.[65] Similar information can be gleaned from the IR spectra of 3-D SAMs: broad bands at high wavenumbers are interpreted to indicate poorly ordered chains having many gauche defects, while sharp bands at relatively low wavenumbers are interpreted to indicate highly ordered chains having predominantly trans zigzag conformations.[65]

Figure 3 presents a summary of the C−H stretches observed for the following samples both in the solid state and dissolved in $CCl_4$: *n*-octadecyl disulfide and 3-D SAMs on gold generated by the adsorption of *n*-octadecyl disulfide and *n*-octadecanethiol. Here, we omit the bands for the free thiol since they are indistinct from those of the free disulfide in this spectral region. Figure 3a shows the IR spectrum of free *n*-octadecyl disulfide in solution, which exhibits $\nu_{as}(CH_2)$ at 2927 $cm^{-1}$ and $\nu_s(CH_2)$ at 2855 $cm^{-1}$. In contrast, however, Figure 3b shows that in the solid state, these bands sharpen and shift to lower wavenumbers: $\nu_{as}(CH_2) = 2919$ $cm^{-1}$ and $\nu_s(CH_2) = 2850$ $cm^{-1}$. By analogy to polyethylene,[65] these changes suggest an ordering (or crystallization) of the methylene chains in the solid state.

Figure 3c shows the C−H stretches for the dissolved 3-D SAMs prepared by the adsorption of *n*-octadecyl disulfide on gold. The stretches appear at $\nu_{as}(CH_2) = 2924$ $cm^{-1}$ and $\nu_s(CH_2) = 2854$ $cm^{-1}$. Comparison of these data to those in Figure 3a of the dissolved free disulfide suggests that the adsorption process induces a faintly detectable ordering of the methylene chains. As shown in Figure 3d, evaporation of the solvent further sharpens and shifts the methylene stretches to $\nu_{as}(CH_2) = 2918$ $cm^{-1}$ and $\nu_s(CH_2) = 2850$ $cm^{-1}$, indicating a further increase in crystallinity.

Parts e and f of Figure 3 present the analogous IR data for dissolved and solid-state 3-D SAMs prepared by the adsorption of *n*-octadecanethiol on gold. The spectra cannot be distinguished from those obtained with the disulfide-based samples (Figure 3c,d). Consequently, these data suggest that 3-D SAMs on gold prepared from *n*-octadecyl disulfide are indistinct from those prepared from *n*-octadecanethiol. Furthermore, the data obtained using the characterization methods described above are consistent with this interpretation.

(65) Snyder, R. G.; Strauss, H. L.; Elliger, C. A. *J. Phys. Chem.* **1982**, *86*, 5145.

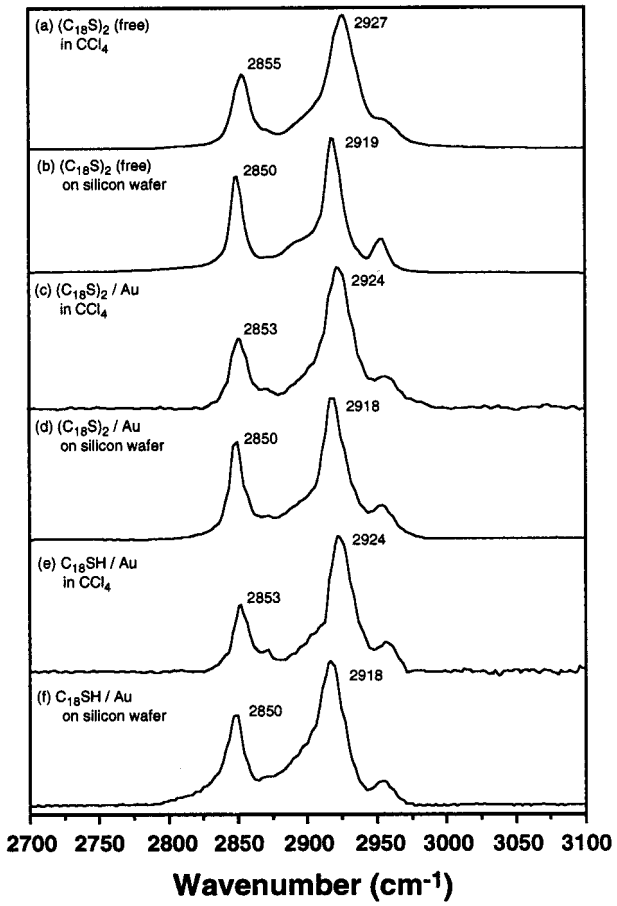


**Figure 3.** FTIR transmission spectra in the 2700−3100 $cm^{-1}$ region for solution ($CCl_4$) and solid-state samples of (a, b) free *n*-octadecyl disulfide, (c, d) gold nanoparticles functionalized with *n*-octadecyl disulfide, and (e, f) gold nanoparticles functionalized with *n*-octadecanethiol.

It is interesting to note that the vibrational frequencies used to judge the degree of crystallinity are the same for all three solid-state samples. The observed increase in crystallinity upon removal of the solvent can arise from at least two plausible processes: (1) loss of solvent from the interchain matrix and (2) increasing interdigitation of neighboring tail groups. While the present data do not distinguish between these processes, it is further interesting to note that the high degree of crystallinity suggested by the solid-state data is comparable to that of high-quality 2-D SAMs of alkanethiols on evaporated gold.[13] Since the latter data were obtained, first of all, from a geometry that excludes interdigitation of neighboring tail groups, and second, in the absence of a contacting solvent, we conclude the high degree of crystallinity observed for solid-state 3-D SAMs on gold arises from an increase in the interchain interactions upon the loss of solvent from the interchain matrix.

Further support for the formation of highly crystalline 3-D SAMs in the solid state was indicated by the appearance of twisting-rocking and wagging progression IR bands between 1180 and 1375 $cm^{-1}$ [46] and the appearance of a sharp scissoring band of the methylene groups at 1470 $cm^{-1}$ for all of the solid-state samples (data not shown).[46] In contrast, the latter band appeared at 1466 $cm^{-1}$ for the free disulfide and the 3-D SAMs dissolved in $CCl_4$. Again, these data argue for a higher degree of crystallinity in the solid state. Additionally, the data are consistent with the interpretation that alkanethiols and dialkyl disulfides form indistinct 3-D SAMs on gold.

**II. 3-D SAMs on Silver Nanoparticles. Solubility of $(C_{18}S)_2$/Ag Nanoparticles.** We briefly probed the solubility of the functionalized silver nanoparticles and found them to dissolve in a wide range of organic solvents (e.g., hexane, cyclohexane, benzene, $CCl_4$, and THF). The particles could be repeatedly precipitated and redissolved, showing no loss of solubility over time. Since bare silver and gold nanoparticles are known to flocculate upon removal of solvent,[33] this observation strongly suggests that the disulfides at least partially coat the surfaces of the nanoparticles.

**TEM Images of $(C_{18}S)_2$/Ag Nanoparticles.** We examined the morphology and size distribution of the disulfide-functionalized silver nanoparticles by TEM. Figure 4a shows that the nanoparticles are slightly elliptical; this type of morphology has been observed previously for alkanethiol-functionalized silver nanoparticles.[50] Analysis of the TEM images afforded a detailed size distribution based on 100 counts. The plot in Figure 4b illustrates that the particles ranged in size from predominantly 4 to 10 nm (with diameters of 6−7 nm occurring most frequently). The plot in Figure 4c shows that the distribution afforded by the thiol is comparable to that of the disulfide. Both distributions are comparable to those reported in the literature in which the data are unbiased by size-selective precipitation methods or other separation techniques prior to analysis by TEM.[66] Furthermore, we observe in separate studies that a doubling of the concentration of the disulfide affords substantially smaller nanoparticles (ca. 4 nm). Taken together, these data support the hypothesis that the sulfur-to-silver ratio (rather than the molecule-to-silver ratio) is the predominant factor controlling the average size of the nanoparticles.[35]

**UV−vis Spectroscopy of $(C_{18}S)_2$/Ag Nanoparticles.** UV−vis spectra of the functionalized nanoparticles exhibited a strong absorption at 475 nm (data not shown). This absorption corresponds to the silver plasmon resonance;[67] the observed frequency is indistinct from that previously reported for alkanethiol-functionalized silver nanoparticles.[68]

**$^1$H NMR Spectroscopy of $(C_{18}S)_2$/Ag Nanoparticles and Nanoparticle Formation.** Analysis of the functionalized silver colloids by $^1$H NMR spectroscopy in $CDCl_3$ showed three broad resonances at 0.8−0.9, 1.2−1.4, and 1.5−1.7 ppm (data not shown). We were unable to detect any resonances attributable to the presence of free alkanethiol (e.g., $\delta$ 2.50 ppm) or free dialkyl disulfide (e.g., $\delta$ 2.67 ppm). These observations suggest that the hydrocarbon species derived from the disulfide are attached to the surface of the colloid via the sulfur atom.[45] Furthermore, the spectra are fully consistent with those reported in the literature for colloidal nanoparticles functionalized with 3-D SAMs derived from alkanethiols.[47]

To test for the possibility that $NaBH_4$ might generate transient thiol which could serve as the active agent in SAM formation, we performed the type of blank $^1$H NMR experiment outlined above for the gold nanoparticles but omitted the $AgNO_3$ (instead of the $HAuCl_4$ as described above). As in the gold case, we were unable to detect the presence of *n*-octadecanethiol. While these studies provide only indirect evidence that the disulfide is the active agent in the formation of 3-D SAMs on silver, the IR studies detailed below provide much stronger support for this hypothesis.

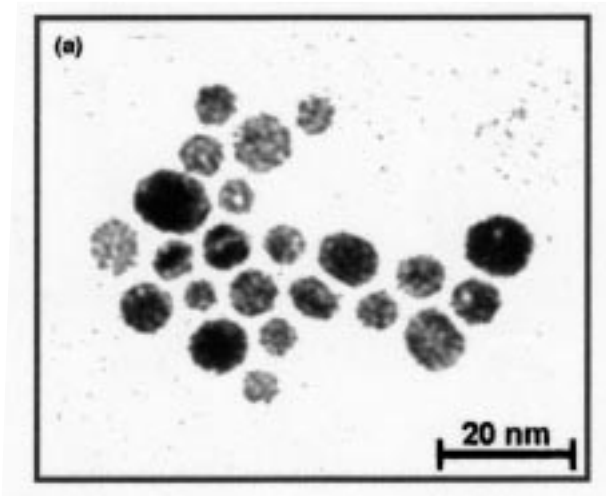


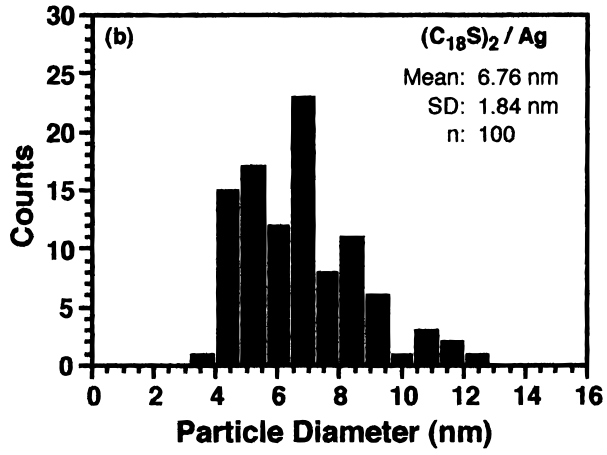


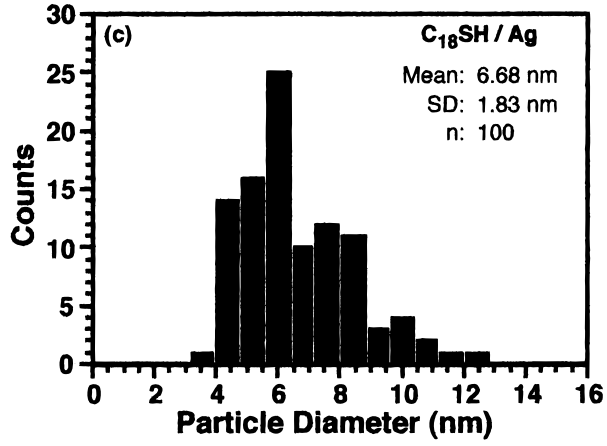


**Figure 4.** (a) TEM image of silver nanoparticles functionalized with *n*-octadecyl disulfide. (b) TEM-derived nanoparticle size distribution for silver nanoparticles functionalized with *n*-octadecyl disulfide. (c) TEM-derived nanoparticle size distribution for silver nanoparticles functionalized with *n*-octadecanethiol.

**Raman Spectroscopy of $(C_{18}S)_2$/Ag and $C_{18}SH$/Ag Nanoparticles.** The characterization of thiol-functionalized silver nanoparticles by Raman spectroscopy has been reported by a number of research teams.[19,20] Bonding of the disulfide to the colloid can be followed by monitoring

(66) Murray, C. B.; Norris, D. J.; Bawendi, M. G. *J. Am. Chem. Soc.* **1993**, *115*, 8706.
(67) Duff, D. G.; Baiker, A.; Edwards, P. P. *Chem. Commun.* **1993**, 96.
(68) Henglein, A. *J. Phys. Chem.* **1993**, *97*, 5457.
(69) Joo, T. H.; Kim, K.; Kim, M. S. *J. Phys. Chem.* **1986**, *90*, 5816.

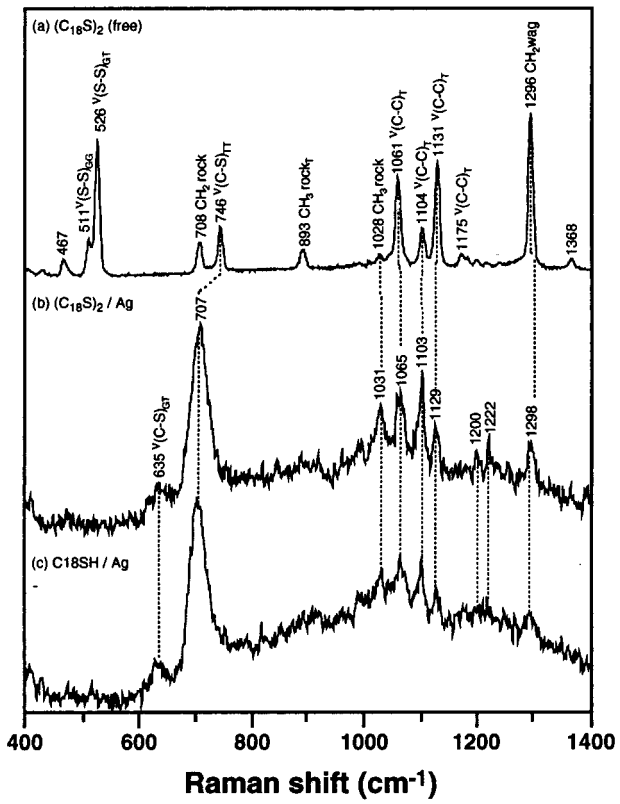


**Figure 5.** Raman spectra in the 600−1400 cm$^{-1}$ region for solid-state samples of (a) free *n*-octadecyl disulfide, (b) silver nanoparticles functionalized with *n*-octadecyl disulfide, and (c) silver nanoparticles functionalized with *n*-octadecanethiol.

the disappearance of the S−S stretch (500−540 cm$^{-1}$) and shifts of the C−S stretches (600−750 cm$^{-1}$). Figure 5 shows the solid-state Raman spectra of *n*-octadecyl disulfide and the 3-D SAMs produced from the adsorption of *n*-octadecyl disulfide and *n*-octadecanethiol on silver colloid. Unadsorbed (or free) *n*-octadecyl disulfide exhibits a strong band at 526 cm$^{-1}$ with a shoulder at 511 cm$^{-1}$ (Figure 5a), which arise from the $\nu$(S−S) stretches of the gauche−trans (GT) and gauche−gauche (GG) conformations, respectively.[61−64] Upon adsorption, these two bands disappear, and two new bands at 707 and 635 cm$^{-1}$ appear (Figure 5b). These new bands also appear with the adsorption of *n*-octadecanethiol onto the silver colloid (Figure 5c). These data provide, to our knowledge, the first direct support for disulfide-based covalent functionalization of silver colloid.

We assign the 707 cm$^{-1}$ SERS band, which shifts from 746 cm$^{-1}$ for the free disulfide, as the $\nu$(C−S) stretch of the trans−trans (TT) conformer; the 635 cm$^{-1}$ band corresponds to the $\nu$(C−S) stretch of the GT conformer (parts b and c of Figure 5). For the free disulfide, the absence of a GT band suggests highly ordered alkyl chains in the region near the sulfur atoms.[62] In contrast, for the 3-D SAMs, the relative intensities of the 707 and 635 cm$^{-1}$ $\nu$(C−S) stretching bands suggest a small concentration of gauche defects in this region.[63] These observations are consistent with reports of relatively large TT/GT ratios for crystalline samples.[63] We were also able to detect the $\nu$(C−S) GT band at 655 cm$^{-1}$ in a sample of the free disulfide dissolved in benzene (data not shown).

While the C−S stretching region provides structural information regarding the portion of the molecule adjacent to the sulfur headgroup, the C−C stretching region provides structural information regarding the more distant carbon skeleton. The free disulfide exhibits three

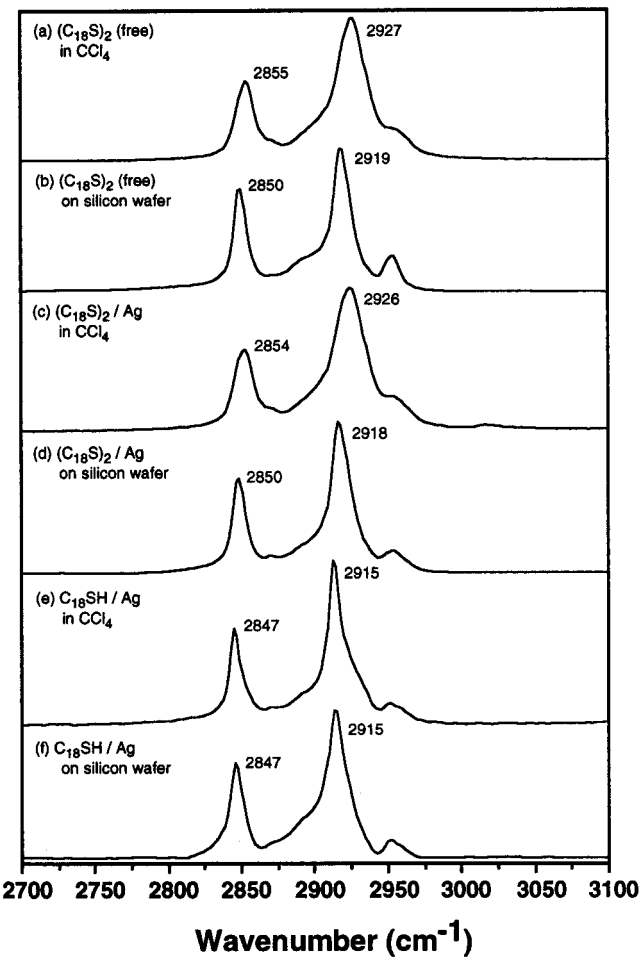


**Figure 6.** FTIR transmission spectra in the 2700−3100 cm$^{-1}$ region for solution ($CCl_4$) and solid-state samples of (a, b) free *n*-octadecyl disulfide, (c, d) silver nanoparticles functionalized with *n*-octadecyl disulfide, and (e, f) silver nanoparticles functionalized with *n*-octadecanethiol.

intense bands in this region (1061, 1104, and 1131 cm$^{-1}$), which we assign as trans $\nu$(C−C) vibrations (Figure 5a). In the 3-D SAMs prepared from both the disulfide and the thiol, we observe a substantial enhancement of the trans $\nu$(C−C) band at 1104 cm$^{-1}$ (parts b and c of Figure 5). Bands located at 1200 and 1222 cm$^{-1}$ also exhibit enhancement as observed previously with SAMs on silver.[63] These data indicate that the SAMs orient with their alkyl chains predominantly normal to the surface. In addition, the absence of gauche $\nu$(C−C) vibrations suggests that the alkyl chains are oriented in trans zigzag conformations.[62]

**IR Spectroscopy of $(C_{18}S)_2$/Ag and $C_{18}SH$/Ag Nanoparticles.** Figure 6 shows the methylene C−H stretching vibrations of the following samples taken both in the solid state and dissolved in $CCl_4$: *n*-octadecyl disulfide and 3-D SAMs on silver generated by the adsorption of *n*-octadecyl disulfide and *n*-octadecanethiol. In this spectral region, the IR bands of the free thiol cannot be distinguished from those of the free disulfide and are thus not shown. The IR spectrum of free *n*-octadecyl disulfide in solution (Figure 6a) shows $\nu_{as}(CH_2)$ at 2927 cm$^{-1}$ and $\nu_s(CH_2)$ at 2855 cm$^{-1}$. In the solid state (Figure 6b), however, the bands sharpen and downshift to $\nu_{as}(CH_2)$ = 2919 cm$^{-1}$ and $\nu_s(CH_2)$ = 2850 cm$^{-1}$. As noted above for polyethylene, these changes are consistent with ordering (or crystallization) of the methylene chains in the solid state.

The solution IR spectrum for the 3-D SAMs prepared from *n*-octadecyl disulfide (Figure 6c) exhibits the following

bands: $\nu_{as}(CH_2) = 2926\ cm^{-1}$ and $\nu_s(CH_2) = 2854\ cm^{-1}$. Comparison of this spectrum to that of the free disulfide in $CCl_4$ (Figure 6a) reveals that the adsorption process induces no detectable ordering of the methylene chains. Evaporation of the solvent, however, sharpens and shifts $\nu_{as}(CH_2)$ to 2918 $cm^{-1}$ and $\nu_s(CH_2)$ to 2850 $cm^{-1}$ (Figure 6d), indicating an increase in crystallinity. The magnitude of the sharpening and shifting of the $CH_2$ bands upon evaporation of the solvent for both the free disulfide and the 3-D SAMs formed from the disulfide are indistinct. These observations therefore suggest that the mechanisms leading to an apparent ordering of the chains of the 3-D SAMs in the solid state are similar in nature to the mechanisms leading to the bulk crystallization of hydrocarbon chains.

The 3-D SAMs prepared by the adsorption of *n*-octadecanethiol, however, exhibit markedly different behavior (Figures 6e and 6f): in both the solid state and in solution, the methylene stretches appear as sharp bands at $\nu_{as}(CH_2) = 2915\ cm^{-1}$ and $\nu_s(CH_2) = 2847\ cm^{-1}$.[70] These features suggest that the 3-D SAMs produced from the adsorption of alkanethiols onto silver are highly crystalline, both in the solid state *and in solution*. Furthermore, the similar shape and frequency for the solid state and solution $\nu(CH_2)$ bands suggest that the crystallinity arises from the self-assembly process rather than from tail-group interdigitation.[45] While we cannot rule out the possibility that clustering (and thus tail-group interdigitation) of the particles occurs to some extent in solution, it seems untenable that this phenomenon would characterize the thiol-derived SAMs but not the disulfide-derived SAMs. Furthermore, our studies of 3-D SAMs on gold derived from either thiols or disulfides show no support for tail-group interdigitation (vide supra). Consequently, for alkanethiol-derived 3-D SAMs on silver, the mechanisms leading to crystallinity must be distinct from those leading to the bulk crystallization of hydrocarbon chains.

Since the solution and solid-state IR spectra of the 3-D SAMs prepared from adsorption of the alkanethiol on silver are identical, one might conclude that these SAMs are more tightly packed than those formed from adsorption of the disulfide on silver. Biebuyck et al. reported that 2-D SAMs generated from the adsorption of disulfides onto gold exhibited contact angles of hexadecane that were 3° lower than those observed on analogous thiol-derived SAMs.[53] Exposure of the disulfide-derived SAM to a solution of the thiol, however, led to a "healing" of the SAM, with limiting contact angles observed.

Using this type of approach, we explored the possibility of "healing" the 3-D SAMs derived from the adsorption of the disulfide on silver. Exposure of these SAMs to a 1 mM solution of *n*-octadecanethiol in toluene for 12 h, however, caused no discernible difference in the IR spectrum (data not shown). Furthermore, we were unable to increase the crystallinity of these disulfide-derived 3-D SAMs by either (1) extending the reaction time from 12 h to either 24 or 48 h or (2) doubling the molar concentration of the disulfide.

The formation of highly crystalline 3-D SAMs in the solid state is further supported by the presence of twisting−rocking and wagging progression bands located between 1180 and 1375 $cm^{-1}$ [46] and the appearance of a sharp scissoring band of the methylene groups at 1470 $cm^{-1}$ for all of the solid-state samples (data not shown).[50] For the free disulfide dissolved in $CCl_4$, the latter band appears at 1466 $cm^{-1}$. For the solution spectra of the 3-D SAMs, this $CH_2$ scissor vibration appears at 1466 $cm^{-1}$ for the disulfide-derived sample and at 1468 $cm^{-1}$ for the thiol-derived sample. Again, these data argue that the SAMs derived from the thiol are slightly more crystalline than those derived from the disulfide.

**XPS of $(C_{18}S)_2$/Ag and $C_{18}SH$/Ag Nanoparticles.** Analyses of SAMs by XPS provides information regarding the atomic composition of thin organic films and their underlying substrates.[71] This technique has been used to characterize thiol-derived 3-D SAMs on gold[72] and silver[22] nanoparticles. In our studies of 3-D SAMs on silver, we felt that XPS might reveal the origin of the observed differences between disulfide-derived and thiol-derived SAMs. A tenable hypothesis centered on the known propensity of silver to form a native oxide coating.[15,16] The adsorption of a disulfide onto such a partially oxidized surface might be disfavored compared to that of a thiol since the thiol moiety might serve as a reducing agent to partially remove the oxide layer from the surface, thereby promoting further adsorption. If this hypothesis were true, the XPS data might be expected to reflect a reduced percentage of oxygen for the thiol-derived 3-D SAMs. While examination of both SAMs by XPS revealed no oxygen in either sample, the predominant sulfur species in the disulfide-derived sample appeared at higher binding energies (e.g., $S_{2p3/2} = 163.1$ eV) than those in the thiol-derived sample (e.g., $S_{2p3/2} = 161.9$ eV) (data not shown). Literature studies of SAMs on evaporated gold have assigned sulfur species with similarly high binding energies as unbound thiol or disulfide.[73] In the present work, we have no independent data to confirm these assignments. We do note, however, that the $^1H$ NMR and Raman spectroscopy studies presented above show no evidence of unbound sulfur species in either sample. Future studies will explore the origin of these differences in greater detail.

## Conclusions

Our studies have demonstrated a new procedure for the preparation of 3-D SAMs on gold and silver nanoparticles. To our knowledge, the studies represent the first use of dialkyl disulfides to effect this type of functionalization. The gold nanoparticles functionalized in this manner exhibited solubilities and size distributions that were comparable to those prepared by the analogous adsorption of alkanethiols. Raman spectroscopy showed that the new 3-D SAMs form by the covalent attachment of the sulfur atoms of the disulfide to the surface of gold. The alkyl chains appeared to be highly ordered in the region near the sulfur headgroup. Analysis by IR spectroscopy revealed that the new 3-D SAMs are indistinct from those prepared via the adsorption of alkanethiols. While the solution-phase adsorption process led to a moderate increase in the crystallinity of the methylene chains of the adsorbate, the subsequent removal of the solvent led to a further increase in crystallinity. The high degree of crystallinity observed in the solid state appears to arise from an increase in the interchain interactions of the SAM upon the loss of solvent from the interchain matrix.

(70) The values observed here for the methylene resonances are lower than those observed for bulk hydrocarbon crystals[63] or for 2-D SAMs on gold or silver.[3,4] At present, we are unable to rationalize this observation. We note, however, that similar low values have been obtained for solid-state samples of 3-D SAMs on silver nanoparticles.[46]

(71) Ulman, A.; Elman, J. F. in *Characterization of Organic Thin Films;* Ulman, A., Ed.; Butterworth-Heinemann: Boston, 1995.
(72) Johnson, S. R.; Evans, S. D.; Mahon, S. W., Ulman, A. *Langmuir* **1996**, *12*, 51.
(73) Castner, D. G.; Hinds, K.; Grainger, D. W. *Langmuir* **1996**, *12*, 5083.

Disulfide-functionalized silver nanoparticles exhibited size distributions and solubilities that were comparable to those of thiol-functionalized silver nanoparticles. Raman spectroscopy showed that the newly derived 3-D SAMs form by the covalent attachment of the sulfur atoms of the disulfide to the surface of silver. The alkyl chains were highly ordered with their molecular axes oriented along the surface normal. IR spectroscopy showed that the newly derived 3-D SAMs were highly crystalline in the solid state but not in solution. In contrast, 3-D SAMs produced by the adsorption of alkanethiols on silver are highly crystalline both in solution as well as in the solid state. While the present studies were unable to pinpoint the origin of these differences, the data nevertheless provided strong support that the adsorbing species in disulfide-derived 3-D SAMs on silver is in fact the disulfide itself rather than the corresponding thiol, which could tenably be generated in small concentration under the reducing conditions employed in the synthesis of the nanoparticles. By inference, this conclusion likely holds as well for the adsorption of disulfides onto gold nanoparticles.

**Acknowledgment.** The National Science Foundation (CAREER Award to T.R.L.; CHE-9625003), the Office of Naval Research (R12671-72000097), the National Aeronautics and Space Administration (96-HEDS-02-088), and the Robert A. Welch Foundation provided generous support for this research. We thank Dr. Paul van der Heide for assistance with the XPS analyses.

LA980870I